Molecular Structures, Tautomerism, and Carbon Nucleophilicity of Free-Base Inverted Porphyrins and Carbaporphyrins: A Density Functional Theoretical Study

Abhik Ghosh,* Tebikie Wondimagegn, and Henning J. Nilsen

Institute of Chemistry, Faculty of Science, University of Tromsø, N-9037 Tromsø, Norway

Received: July 14, 1998; In Final Form: September 14, 1998

Using geometry optimizations with nonlocal density functional theory, we have carried out a broad survey of the molecular structures of porphyrin variants including inverted porphyrin, true carbaporphyrin, azuliporphyrin, and oxacarba- and thiacarbaporphyrins. For each ring system studied, we have calculated the relative energies of different tautomeric forms and the energies have been correlated with structural features of the central region of the macrocycles such as hydrogen-bonding interactions and hydrogen−hydrogen repulsions. The molecular geometry of azuliporphyrin, which is not available from experiment, provides an interesting illustration of the structural effect of intersecting [10]- and [18]annulene substructures that are present in this molecule. We propose that the energies of the carbenic tautomers of these molecules are related to their ability to form metal complexes with metal−carbon bonds. Finally, the energetics of carbon nucleophilicity of these molecules is examined by calculating the energies of protonation at various carbon centers. By this measure, we find that the central carbon is the most nucleophilic carbon atom for all the molecules examined. This is consistent with available experimental data on the regioselectivity of electrophilic substitution of inverted porphyrins.

1. Introduction

A variety of structurally modified porphyrins including porphyrin isomers, heteroatom-substituted porphyrins, and expanded and contracted porphyrins have been synthesized in recent years.[1] Among these porphyrin variants, inverted or N-confused porphyrins are of particular interest since they form metal complexes with metal−carbon bonds under mild conditions (Figure 1).[2,3] Structurally related to the inverted porphyrins are the true carbaporphyrins[4] for which metal complexation remains an interesting but as yet unrealized possibility. Theoretical studies have been carried out to understand the carbon acidity and metal-complexing ability of inverted porphyrins.[5] We have proposed that a key factor underlying these properties is that the ligand in metal-complexed inverted porphyrins (Figure 1) may be regarded as a heteroatom-stabilized nucleophilic singlet carbene.[6] Another factor contributing to the ease of the Ni(II) complexation reaction shown in Figure 1 is that there should be a highly favorable covalent interaction between the central carbon of the inverted porphyrin and the empty d_σ orbital of the d_8 Ni^{2+} ion in a square planar ligand field. More incisive quantum chemical studies of this chemistry can certainly be expected in the foreseeable future.

Developing a "feel" for the energetics of various tautomeric forms of inverted porphyrin and carbaporphyrins is necessary for a proper understanding of the interaction of these ligands with transition metals. Here we present density functional calculations on various tautomers of inverted porphyrins, carba-, oxacarba-, and thiacarbaporphyrins and explain the energetics of the different species in terms of their optimized structures. We have also investigated the relative nucleophilicity of the different carbon atoms of inverted and carbaporphyrin molecules using protonation as the simplest example of an electrophilic addition. In particular, we sought to determine whether the central carbon atoms exhibit any enhanced nucleophilicity compared to the other carbon atoms of these ligands. The calculated results are related to the experimentally known properties of these compounds.

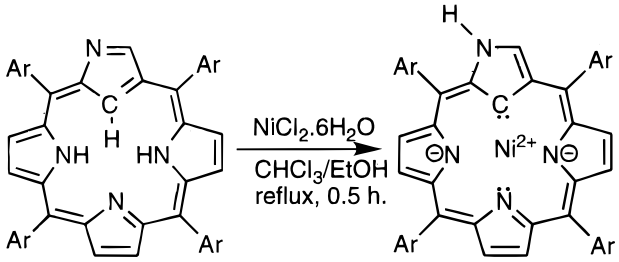

Figure 1. Complexation of Ni(II) by an inverted porphyrin under mild conditions. Note that the product may be formally regarded as a metallocarbene.

2. Methods

All calculations described here employed nonlocal density functional theory (DFT) as implemented in the ADF program system.[7] We used the VWN[8] local exchange-correlation functional, the Perdew−Wang 1991[9] nonlocal corrections, valence triple-ζ plus polarization Slater-type basis sets, a fine mesh for numerical integration of matrix elements, and full geometry optimizations.[7] This and comparable levels of theory have provided generally excellent descriptions of many aspects of porphyrin chemistry[10] such as NH tautomerism in porphyrins,[11] porphyrin[12] and corrole[13] isomers, hydroporphyrins,[14] porphyrin cation radicals,[15] and ionization potentials of porphyrins.[16]

3. Results and Discussion

3A. Energetics of Inverted Porphyrin Tautomers. Figure 2 shows the different tautomeric forms of inverted porphyrin

* Author to whom correspondence should be addressed. Fax: (+47)-77644765. E-mail: abhik@chem.uit.no.

10.1021/jp983010j CCC: $15.00
Published on Web 11/17/1998

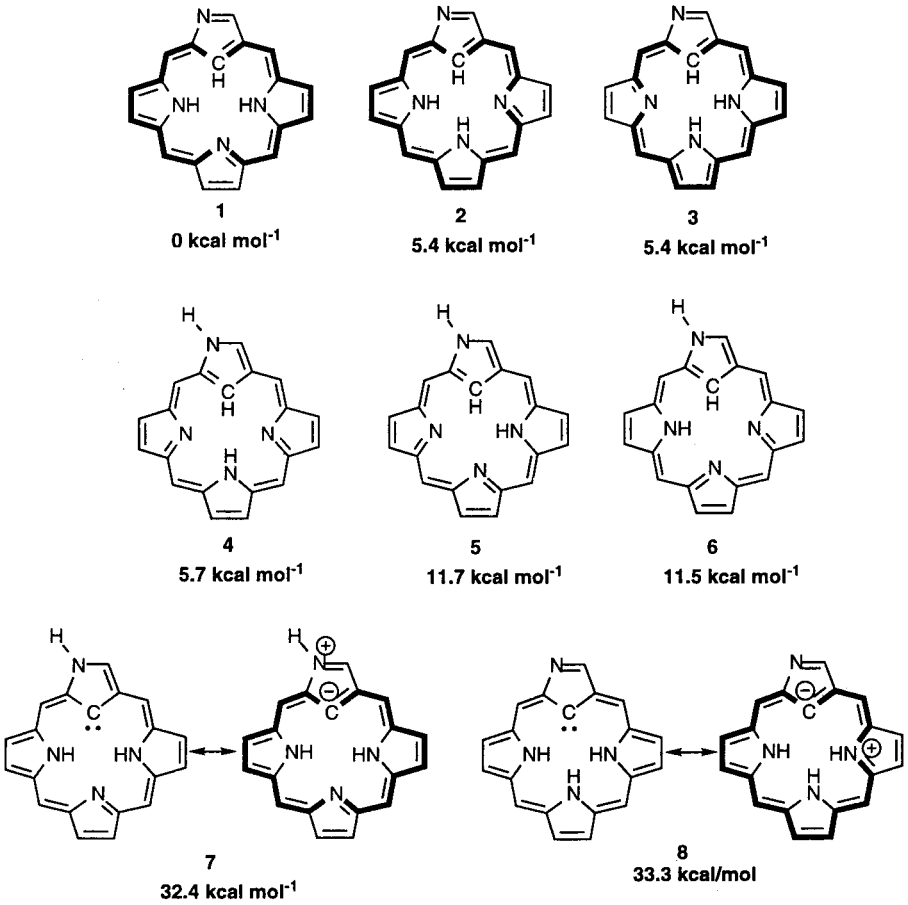

Figure 2. Tautomers of inverted porphyrins and their relative energies.

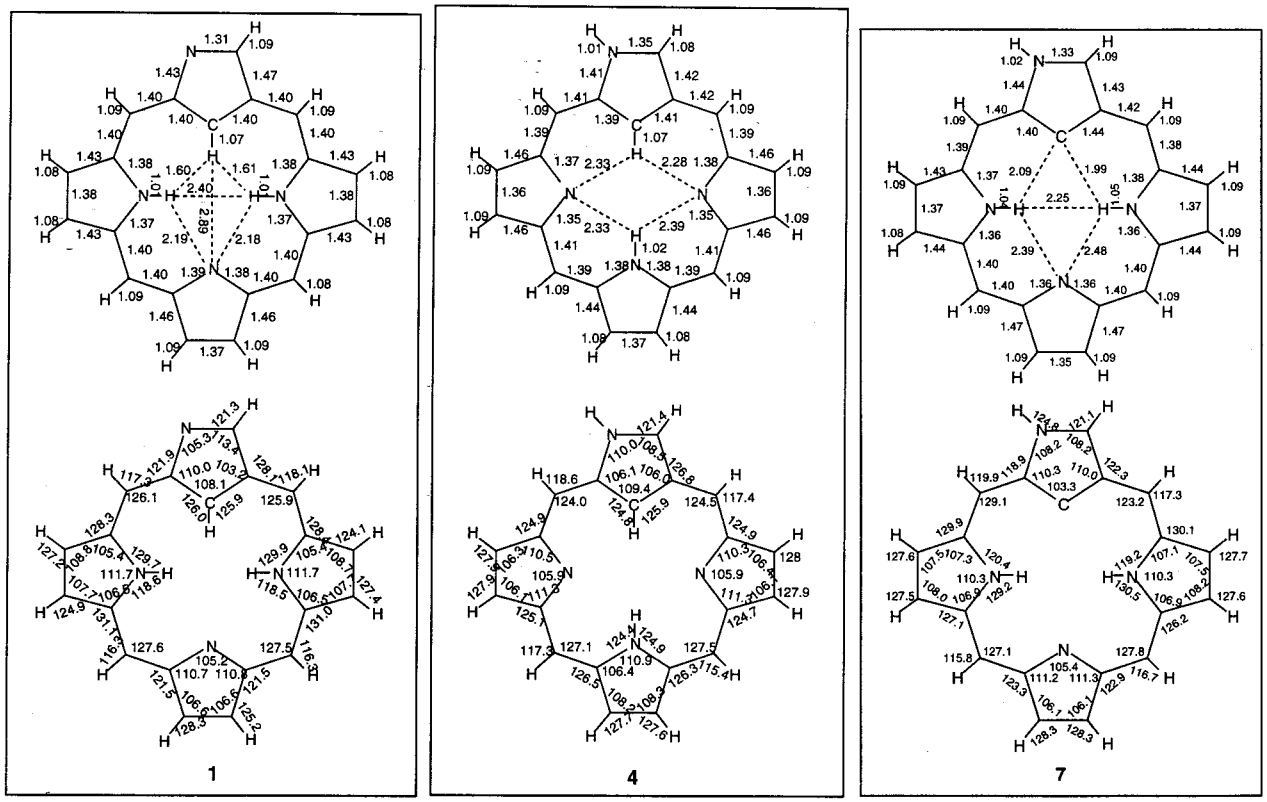

Figure 3. Optimized molecular geometries (Å, deg) of selected inverted porphyrin tautomers.

that we have studied and the relative energies of their optimized structures. For simplicity, each optimization used a C_s symmetry constraint because only small amounts of energy on the order of 1 kcal/mol were found to be associated with moderate buckling of the ring systems investigated here.

The most stable tautomeric form **1** has three central hydro-

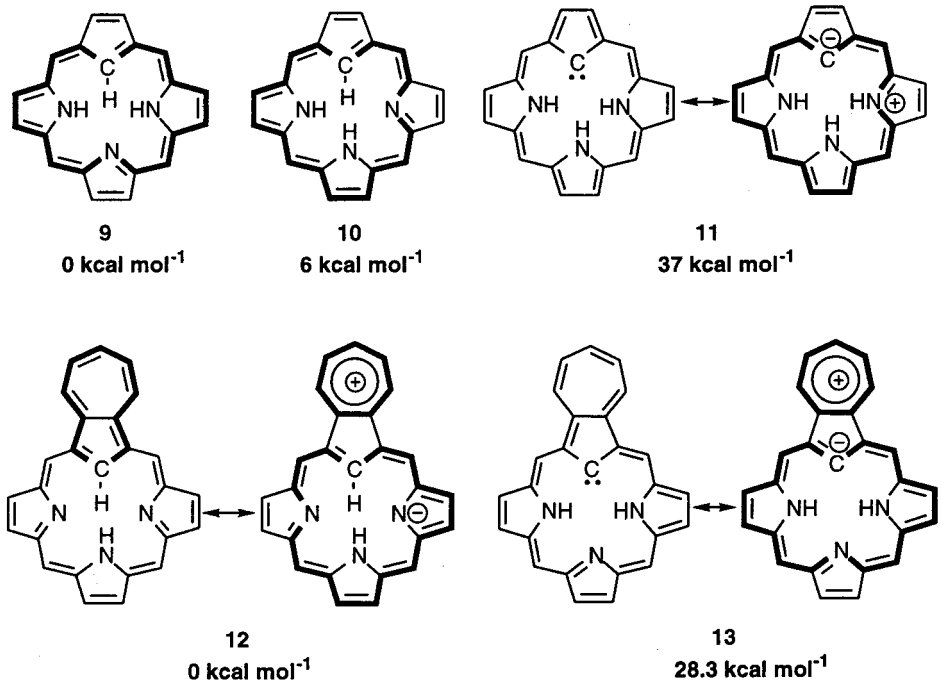

Figure 4. Tautomers of ordinary carbaporphyrin and azuliporphyrin and their relative energies.

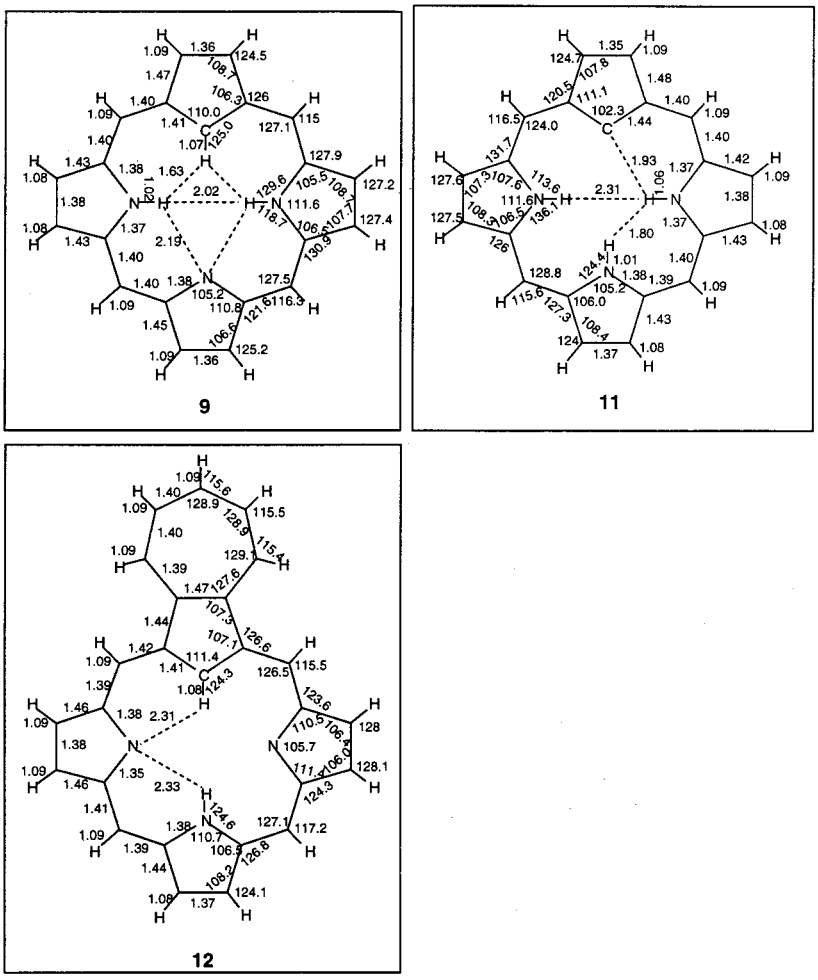

Figure 5. Optimized molecular structures (Å, deg) of tautomers of ordinary carbaporphyrin and of azuliporphyrin.

gens, one of which is attached to the central methine carbon and the other two to the nitrogens closest to the central methine unit. Compared to ordinary porphyrin, **1** has a relative energy of 17.7 kcal mol^{-1}. Part of this energy must be ascribed to the steric repulsions among the three central hydrogens of **1**. Both of the central NHs of **1** are hydrogen-bonded, which should be a factor stabilizing **1** over its tautomer **4**, the latter having an exocyclic NH that is not hydrogen-bonded. In addition, unlike

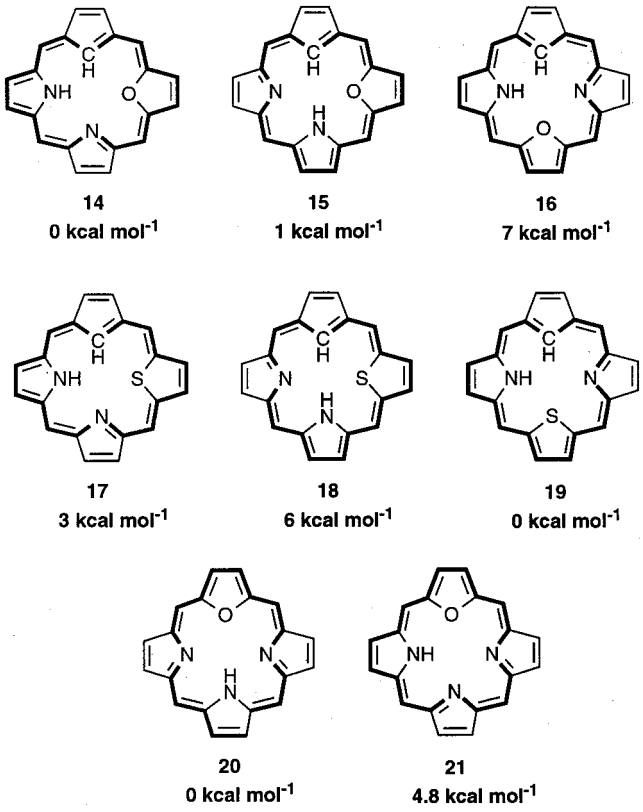

Figure 6. Isomers of oxacarbaporphyrins and thiacarbaporphyrins and their relative energies.

1, the nonzwitterionic resonance form of **4** that is shown in Figure 2 does not have an [18]annulene substructure. Thus, it may seem surprising that **4** is only 5.7 kcal/mol higher than **1**.[17] A reason for this is that **4** has a relatively unencumbered central region with only two hydrogens.

Like **1**, tautomers **2** and **3** contain [18]annulene substructures and are each only about 5 kcal/mol higher in energy than **1**, this energy difference presumably reflecting the fact that only one of the central NHs is hydrogen-bonded in **2** and **3**. Like **4**, tautomers **5** and **6** have only one hydrogen-bonded central NH and no [18]annulene substructure in their nonzwitterionic resonance forms. They differ from **4** in having a cis orientation of the central protons, which explains their moderately high energies of about 11−12 kcal/mol relative to **1**.

Figure 3 shows optimized molecular structures of selected inverted porphyrin tautomers. Most of the geometrical parameters of the structures are unremarkable. Thus, the standard order of bond lengths in ordinary porphyrin holds quite well for inverted porphyrin and other molecules studied in this work. This order is: $C_\alpha-C_\beta$ (1.42−1.46 Å), $C_{meso}-C_\alpha$ (∼1.39 Å), $C_\alpha-N$ (∼1.37 Å), and $C_\beta-C_\beta$ (1.35−1.37 Å).[18] The geometry of the inverted ring of **1** exhibits certain special features. The two $C_\alpha-N$ bonds in the inverted ring of **1** are very unequal (1.31 and 1.43 Å), as are the two $C_\alpha-C_\beta$ bonds. In other words, the bonds in the inverted ring are similar in length to bonds in analogous positions in the normal or uninverted pyrrole rings. A couple of comments are in order on the hydrogen bonds in **1**. The $C_\alpha-N-H$ angles at each NH in **1** are very unequal, a consequence of repulsion between the central CH and each central NH. However, in spite of this distortion, each N−H··· N contact in **1** is about 2.19 Å, which is only slightly shorter than that in ordinary porphyrin (2.31 Å).

A comparison of the optimized structures of **1** and **4** shows that a $C_\alpha-N$ bond and a $C_\alpha-C_\beta$ bond in the inverted ring of **4** are significantly longer and shorter, respectively, than analogous bonds in **1**. This is a structural consequence of the external nitrogen being protonated in **4**. The fact that the $C_\alpha-C_\beta$ bonds are slightly longer in N-unprotonated pyrrole rings than in N-protonated pyrrole rings in free-base porphyrins is an analogous effect.[18] Another way of rationalizing this structural

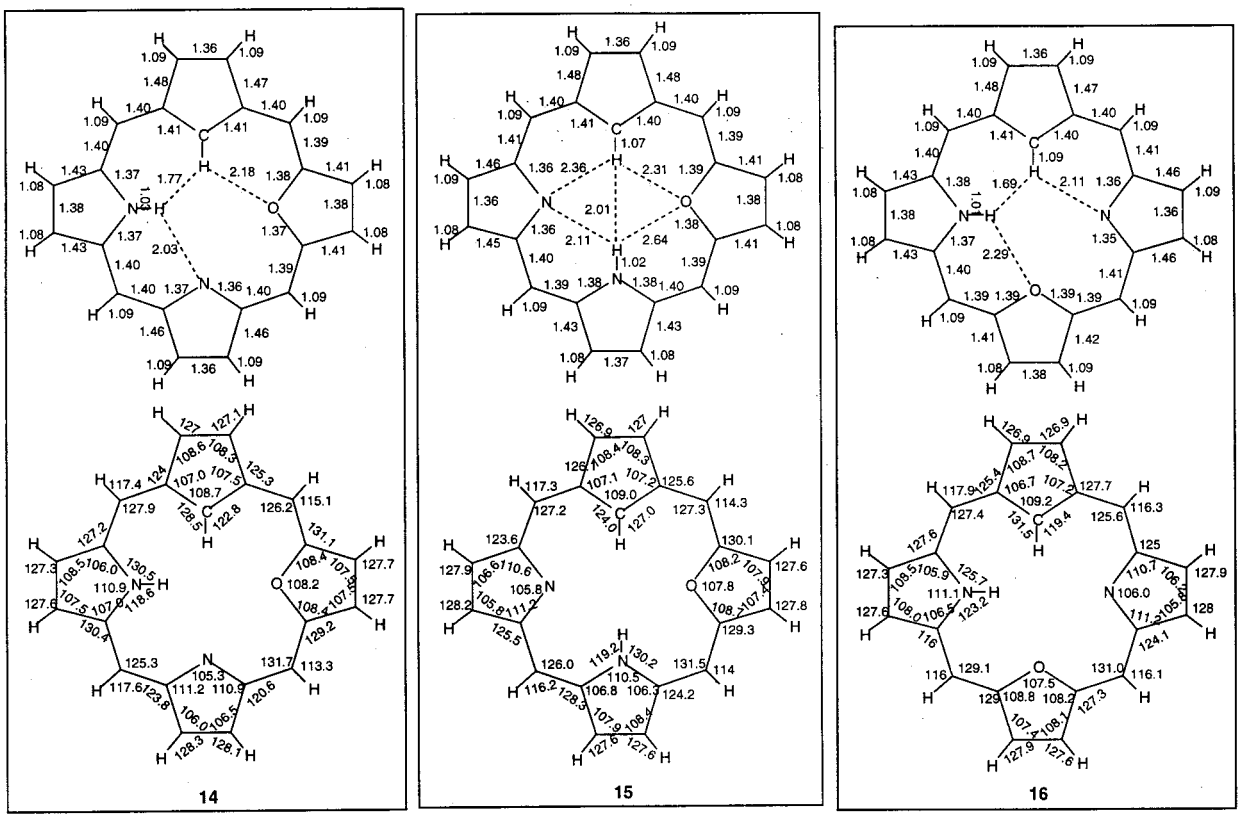

Figure 7. Optimized geometries (Å, deg) of oxacarbaporphyrins.

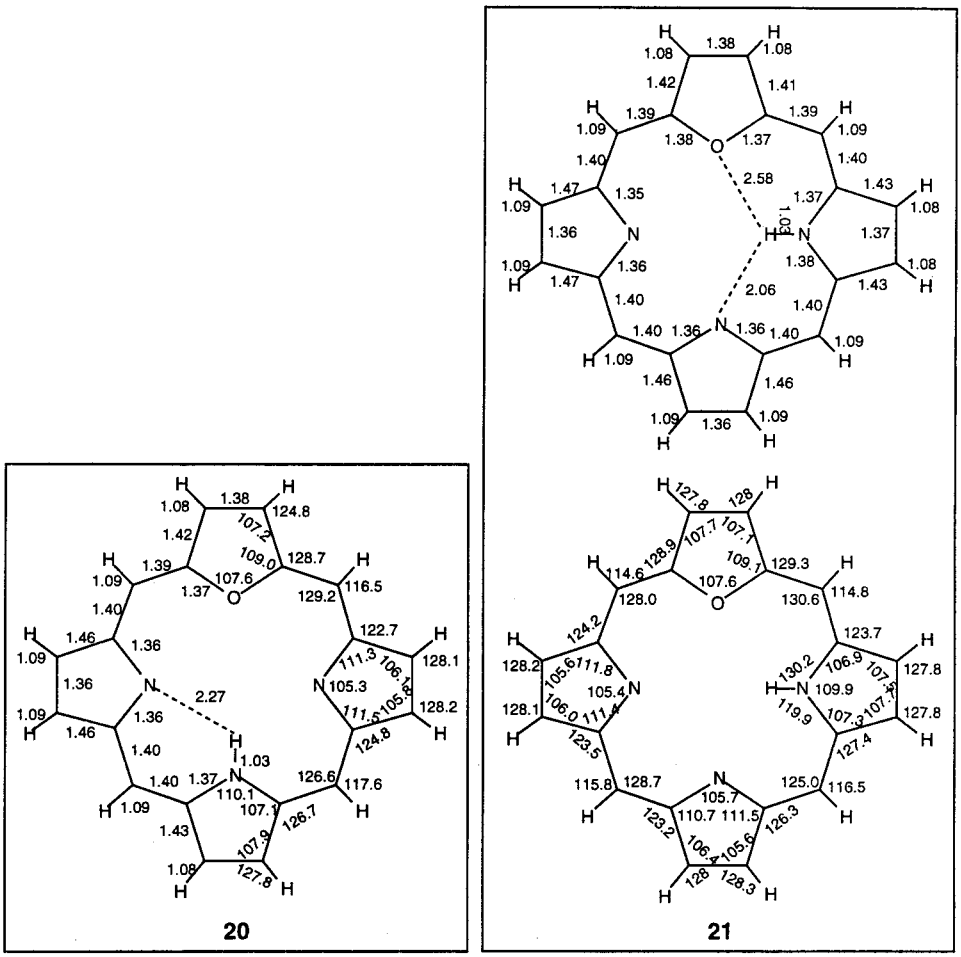

Figure 8. Optimized structures (Å, deg) of oxaporphyrins.

feature is that the $C_\alpha-N$ and $C_\alpha-C_\beta$ bonds in question are formally double and single bonds, respectively, in the resonance form shown for **1**, but single and double bonds, respectively, for **4** (Figure 3).

The nickel inverted porphyrin shown in Figure 1 may be considered to be derived from the carbenic tautomer **7** shown in Figure 2. The energy of **7** at 32.4 kcal/mol relative to **1** is high compared to tautomers **2**−**6**, but is quite moderate considering its carbenic nature. The nonionic resonance form of **7** does not have an [18]annulene substructure but its ionic resonance form shown in Figure 2 does. Theoretical calculations of singlet−triplet splittings and ionization potentials have shown that **7** is electronically similar to heteroatom-stabilized nucleophilic singlet carbenes such as the "bottleable" imidazol-2-ylidenes.[19] This led us to argue that the moderate energy of **7** provides a partial explanation of the carbon acidity and metal-complexing ability of inverted porphyrins. Tautomer **8**, another possible carbenic tautomer, has about the same energy as **7**. By comparison, the carbenic tautomer of pyridine, 1-hydro-2-dehydropyridine, also called the Hammick intermediate, is about 47 kcal/mol above pyridine.[20]

3B. Energetics and Structures of Carbaporphyrin Tautomers. Figure 4 shows various tautomers of a true carbaporphyrin[4a] (i.e., not an inverted porphyrin) and of azuliporphyrin.[21] All of these species were studied with C_{2v} symmetry-constrained optimizations except **10**, which was assumed to be C_s. For the true carbaporphyrin ring system, **9** is the most stable tautomer as a result of the stabilization due to two N−H···N hydrogen bonds. By comparison, **10** has only one hydrogen bond. Molecule **12** is clearly the preferred tautomer of azuliporphyrin, since a tautomer with an N-protonated pyrrole ring adjacent to the "carbapyrrole" ring would be disfavored by CH···HN steric repulsion.

There are important similarities between the energetics and geometrical data on carbaporphyrins shown in Figures 4 and 5 and similar data on inverted porphyrins shown in Figures 2 and 3. The difference in energy between tautomers **9** and **10** in Figure 4 is 6 kcal/mol, essentially the same as the difference between tautomers **1** and **2**. The N−H···N hydrogen bonding distances in **1** and **9** are each 2.19 Å. The $C_\alpha-N-H$ angles are also similar in **1** and **9**. The $C_\alpha-C_\beta$ and $C_\beta-C_\beta$ bonds (α and β being counted off the central CH) in the carbapyrrole ring of **9** are similar in length to analogous bonds in a normal porphyrin. Finally, **9** and its carbenic tautomer **11** differ in energy by 37 kcal/mol, which is slightly higher than the difference in energy between analogous structures **1** and **8**.

Preliminary efforts to prepare metal complexes of **9**, reportedly, have not succeeded.[4a] It is interesting to consider whether this results from the slightly higher relative energy of carbenic tautomer **11** (37 kcal/mol) compared to the carbenic tautomer **7** (32 kcal/mol) of inverted porphyrin. However, we believe that it is more likely that the observed lack of metal complexation by **9** is related to the requirement of dissociation of three protons compared to only two for **1** (note that the metal complex in Figure 1 has two protons less than the free base). We are examining this difference in chemical behavior between **1** and **9** in ongoing calculations in our laboratory.

The carbenic tautomer **13** of the azuliporphyrin has a surprisingly low energy of 28 kcal/mol relative to the stable tautomer **12**. The stability of **13** presumably reflects the

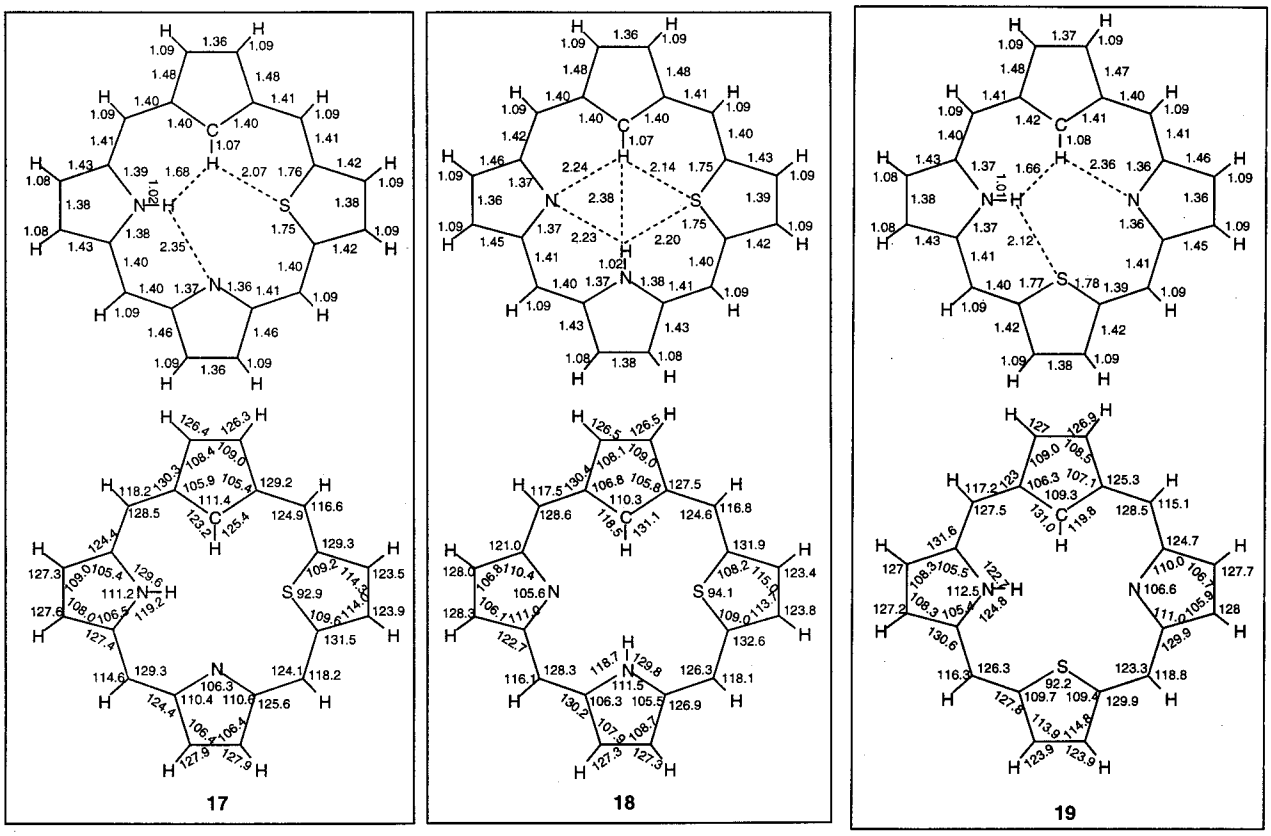

Figure 9. Optimized structures (Å, deg) of thiacarbaporphyrins.

presence of [18]annulene and tropylium substructures in its zwitterionic resonance form shown in Figure 4. Using the same logic as in the case of inverted porphyrins, azuliporphyrin appears to be a good candidate for metal-complexation reactions involving ionization of the central CH bond. This proposal remains to be experimentally checked.

The optimized geometry of **12** reveals moderate bond-length alternation in the carbaporphyrin macrocycle. Note, for instance, significantly unequal lengths of adjacent $C_\alpha-C_{meso}$ bonds and, in the N-unprotonated pyrrole rings, of adjacent $C_\alpha-N$ bonds. Another significant structural feature is the long (1.47 Å) $C_\beta-C_\beta$ ring-fusion bond in the azulene part of **12**. The length of this bond suggests that tropylium-type aromaticity is not important. Instead, it underscores the importance of the [10]-annulene substructure, which must interfere with porphyrin-type aromaticity. Experimental results by Lash and Chaney[21] nicely complement these theoretical findings. Thus, azuliporphyrin does not exhibit a strong Soret band that is typical of porphyrin-type aromatics. The central methine proton also has an NMR chemical shift of $\delta = 1.5$ ppm, which is high for a proton located in the internal cavity of a porphyrin-type aromatic molecule. These results provide an early view of the structural and electronic consequences of intersecting [10]annulene and [18]-annulene substructures in molecule **12**. Additional studies of the electronic structure of **12** are currently in progress in our laboratory.

3C. Energies and Structures of Oxa- and Thiacarbaporphyrin Tautomers. Oxa- and thia-analogues of inverted porphyrins have been recently synthesized.[22] Here we have examined structures and NH tautomerism of oxa- and thiacarbaporphyrins. These calculations were motivated by the possibility that like other oxa- and thiaporphyrins, the molecules shown in Figure 6 may turn out to be interesting transition metal ligands.[1b]

Figure 6 shows different isomers and tautomers of oxa- and thiacarbaporphyrins. The most stable oxacarbaporphyrin structure, **14**, is stabilized by an N−H···N hydrogen bond and destabilized, relative to **15**, by a CH···HN repulsion. Relative to **14**, **15** is stabilized by a less-crowded interior region that has two protons in a trans orientation as opposed to two cis central protons in **14**. However, the manner in which these and other factors balance each other is not clear, and a precise reason cannot be given for the comparable energies of **14** and **15**.

Molecule **16**, a regioisomer of **14** and **15**, has a clearly higher energy of 7 kcal/mol relative to **14**. Isomers **14** and **16** are sterically similar but differ in having N−H···N and N−H···O hydrogen bonds, respectively. In these molecules, an N−H···O hydrogen bond is weaker than an N−H···N bond, which explains the higher energy of **16**. The weakness of the N−H···O interaction can be seen in the optimized structure of **15** (Figure 7), where the NH proton tilts preferentially toward the nitrogen on the adjacent pyrrole ring rather than toward the oxygen in the adjacent furan ring. This appears to be a fairly general trend that also explains the stability of oxaporphyrin tautomer **20** relative to **21** (Figure 6). Tautomer **20** has a symmetrical bifurcated $N-H\cdots N_2$ hydrogen bond system, whereas **21** has an unsymmetrical bifurcated N−H···NO system. As in **15**, the NH proton in **21** tilts toward the nitrogen in the adjacent pyrrole ring rather than toward the oxygen (Figure 8).

The stabilities of the thiacarbaporphyrin structures appear to be dominated by the relatively large size of the sulfur atom: the C−S bonds in thiacarbaporphyrins are about 1.75 Å (Figure 9). Although molecule **18** has a relatively uncrowded trans arrangement of the central protons, it is significantly higher in energy than **17** and **19** which have cis central protons. The reason is that **18** has two protons approaching the large sulfur atom whereas **17** and **19** have each only one S···H contact. The reason why **17** is less stable than **19** is less clear. One possible

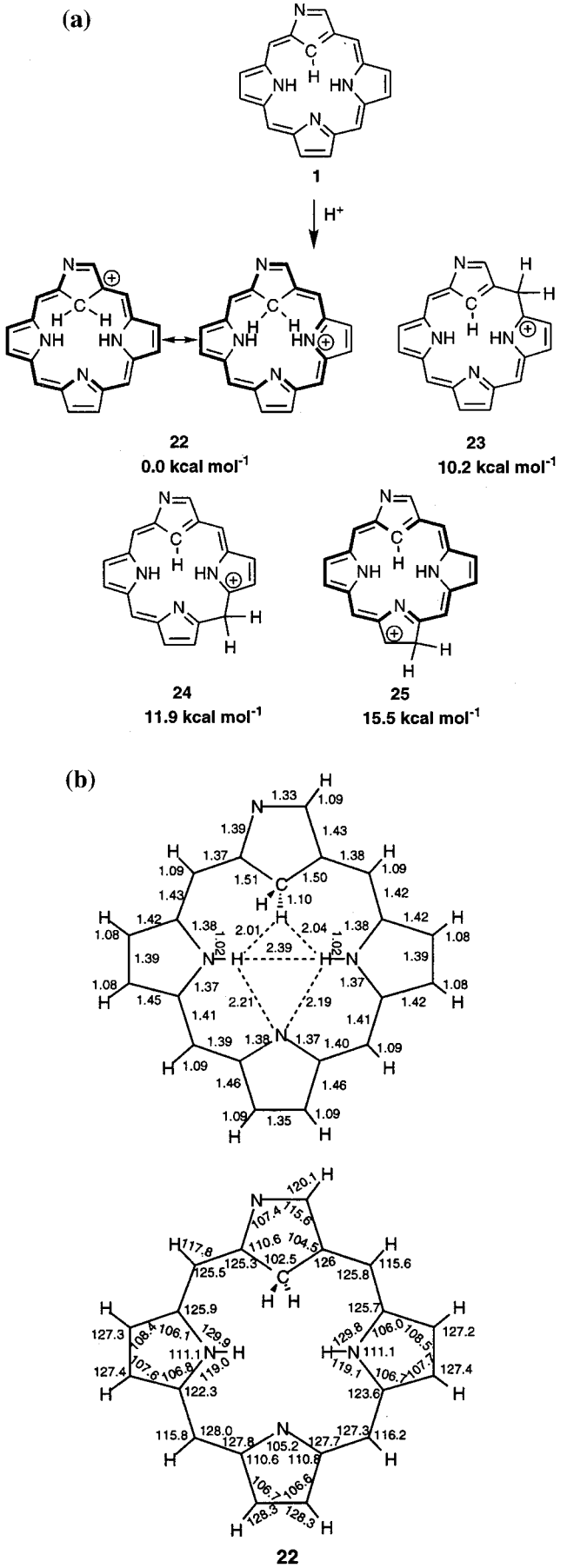

Figure 10. (a) Energetics of protonation of inverted porphyrin for different carbon atoms. (b) Optimized geometry of the most stable C-protonated form of inverted porphyrin.

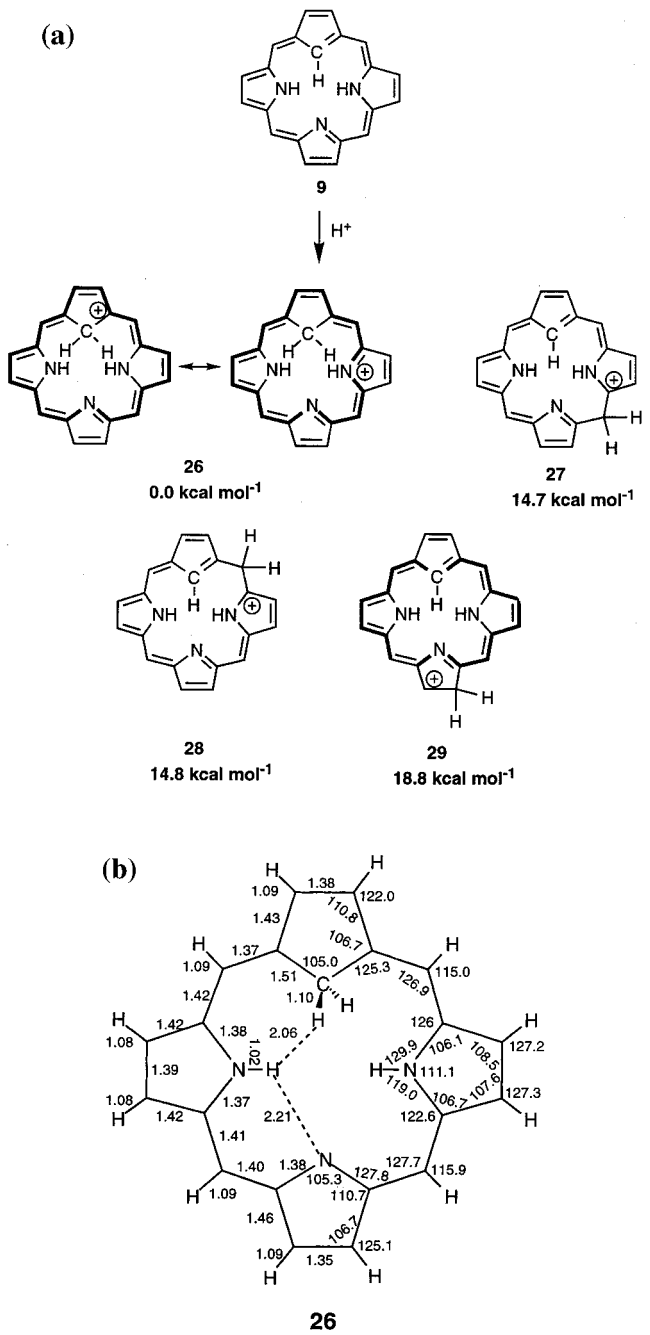

Figure 11. (a) Energetics of protonation of ordinary carbaporphyrin at different carbon atoms. (b) Optimized geometry of the most stable C-protonated form of ordinary carbaporphyrin.

factor is that the NH···S interaction in **19** is more stabilizing than the CH···S interaction in **17**.

3D. Protonation of N-Confused and True Carbaporphyrins. The remarkable metal-complexing ability[2] of inverted porphyrins involving dissociation of the central CH group invites the question whether the central carbon of carbaporphyrins is particularly nucleophilic. We have addressed this question computationally by comparing the nucleophilicity of the central carbon with that of the other carbon atoms in the various carbaporphyrins studied. We have chosen protonation as our model electrophilic addition reaction.

Figure 10a shows various isomeric C-protonated inverted porphyrins along with the energies of their optimized structures relative to the most stable structure, **22**. Intermediate **22**, which results from protonation of the central methine unit, has many

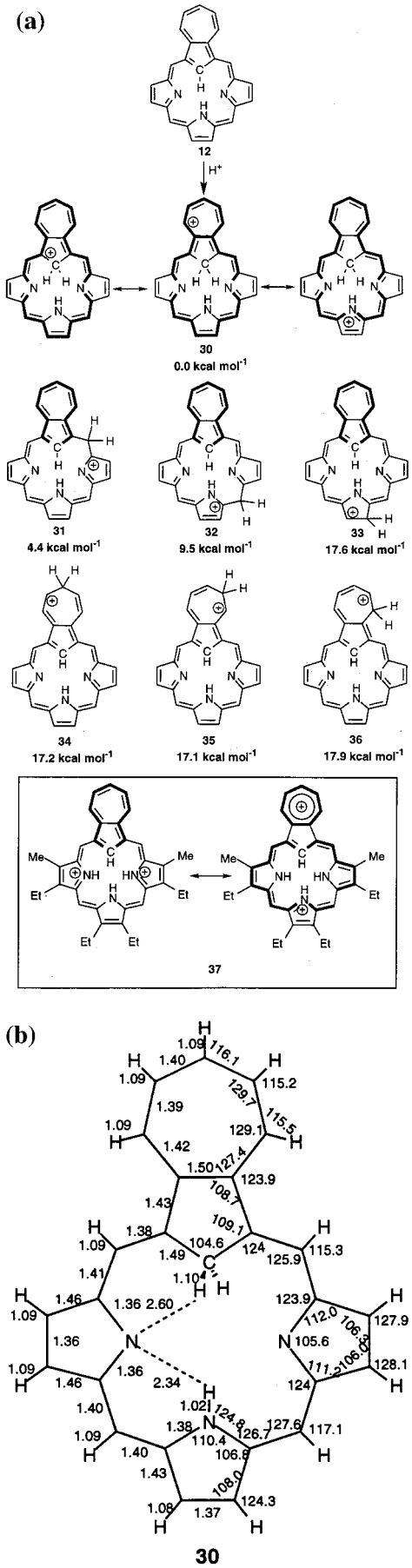

Figure 12. (a) Energetics of protonation of azuliporphyrin at different carbon atoms. (b) Optimized geometry of the most stable C-protonated form of azuliporphyrin.

highly favorable [18]annulene resonance forms. In contrast, the cationic intermediate **25** arising from electrophilic addition to a β C−H has only one [18]annulenic resonance form and a number of relatively unfavorable resonance forms with cross-conjugated non-[18]annulenic structures (not shown), which explains the relatively high energy of this species compared to **22**. Protonation at meso carbons interrupts the aromaticity of the macrocycle, which accounts for the relatively high energies of intermediates **23** and **24**. As shown in Figure 11a, C-protonation of true carbaporphyrin **9** is also preferred at the central methine unit for essentially the same reasons as described above for inverted porphyrins. Figures 10b and 11b show the optimized structures of the most stable C-protonated species **22** and **26**. Special features of these structures are the expected long CH_2-C_α bonds in the carbapyrrole rings, which have lengths typical of single bonds. Consistent with the above description, the geometries of these cationic intermediates are also typical of porphyrin-type aromatics and show only mild bond-length alternation.

Protonation of azuliporphyrin **12**, shown in Figure 12a, is also preferred at the inner methine carbon. This is due to the many [22]annulene resonance forms that are possible for the resulting cation, **30**. The optimized geometry of **30**, shown in Figure 12b, shows that the ring-fusion C−C bond in the azulene part of the molecule has a typical single-bond length of 1.50 Å, showing that this bond is not involved in either [18]annulene or tropylium-type circuits but merely bridges two carbons in a [22]annulene structure. Protonation at the meso position interrupts porphyrin-type aromaticity, but preserves the [10]-annulenic azulene substructure. As seen for inverted porphyrin and true carbaporphyrin, protonation at a β-carbon gives rise to a relatively less stable carbocation **33**. Cations **34**−**36**, resulting from protonation of the seven-membered ring, have no aromatic substructures and, understandably, relatively high energies of 17−18 kcal/mol relative to **30**.

Experimental characterization of **30** may appear to be an intriguing possibility. However, in practice, protonation of azuliporphyrin[21] leads to the N,N′-diprotonated species **37** shown in Figure 12a which exhibits both [18]annulenic and tropylium-type aromaticity, as evidenced by its NMR properties.

Overall, for all three carbaporphyrin structures studied, **1**, **9**, and **12**, the central carbon is clearly more nucleophilic than all other carbon atoms. This implies that electrophilic monosubstitution of carbaporphyrins may be expected to be highly regioselective at the central carbon. Thus, nitration of free-base inverted tetraphenylporphyrin[23] under relatively mild conditions yielded the 21-nitro-substituted derivative as the only isolated product. Additional electrophilic substitution reactions of various carbaporphyrins need to be carried out to test the generality of our prediction.

4. Conclusion

1. Using geometry optimizations with nonlocal density functional theory, we have determined the relative energies of different tautomers of inverted porphyrin, carbaporphyrin, and certain related ring systems. The energies are correlated with structural features such as hydrogen-bonding interactions, H···H repulsions, and the presence or absence of $[4n + 2]$ π-electron substructures.

2. The optimized structure of azuliporphyrin provides an interesting illustration of the structural effects of intersecting [18]annulene and [10]annulene substructures.

3. We have proposed that the stabilities of the carbenic tautomers of the different molecules studied are linked to their

ability to form metal complexes with metal−carbon bonds. By this measure, azuliporphyrin is predicted to be a good candidate for a successful metal complexation reaction.

4. Using protonation as a model electrophilic addition reaction, we have shown that the central carbon is the most nucleophilic carbon in the inverted porphyrin, carbaporphyrin, and azuliporphyrin molecules. This agrees with the experimental observation that inverted porphyrin undergoes nitration regiospecifically at the central carbon.

5. Finally, it is interesting to speculate what the future holds for theoretical studies of this area. Some interesting aspects of these molecules that have not been examined in depth so far include modeling of metal insertion reactions of carbaporphyrins including characterization of "sitting-atop" and other intermediates and detailed characterization of hydrogen bonding, charge distribution, NMR properties, and aromaticity of these compounds.

Acknowledgment. This work was supported by the Research Council of Norway, the VISTA program of Statoil (Norway), and a Senior Fellowship of the San Diego Supercomputer Center (AG). A.G. thanks Prof. Peter Taylor for his hospitality during a sabbatical period spent with his group.

References and Notes

(1) (a) Sessler, J. L.; Weghorn, S. J. *Expanded, Contracted & Isomeric Porphyrins*; Pergamon/Elsevier: Wiltshire, U.K., 1997. (b) Vogel, E. *J. Heterocycl. Chem.* **1996**, *33*, 1461.

(2) (a) Chmielewski, P. J.; Latos-Grazynski, L.; Rachlewicz, K.; Glowiak, T. *Angew. Chem., Int. Ed. Engl.* **1994**, *33*, 779. (b) Furuta, H.; Asano, T.; Ogawa, T. *J. Am. Chem. Soc.* **1994**, *116*, 767. (c) Chmielewski, P. J.; Latos-Grazynski, L.; Glowiak, T. *J. Am. Chem. Soc.* **1996**, *118*, 5690. (d) Liu, B. Y.; Brückner, C.; Dolphin, D. *Chem. Commun.* **1996**, 2141.

(3) Nilsen, H. J.; Ghosh, A. *Acta Chem. Scand.* **1998**, *52*, 827.

(4) (a) Berlin, K. *Angew. Chem., Int. Ed. Engl.* **1996**, *35*, 1820. (b) Berlin, K.; Steinbeck, C.; Breitmaier, E. *Angew. Chem., Int. Ed. Engl.* **1996**, 336.

(5) Ghosh, A. *Angew. Chem., Int. Ed. Engl.* **1995**, *34*, 1028.

(6) For a review of nucleophilic carbenes, see Regitz, M. *Angew Chem., Int. Ed. Engl.* **1996**, *35*, 725.

(7) The ADF program is obtainable from Scientific Computing and Modelling, Department of Theoretical Chemistry, Vrije Universiteit, 1081 HV Amsterdam, The Netherlands.

(8) Vosko, S. H.; Wilk, L.; Nusair, M. *Can. J. Phys.* **1980**, *58*, 1200.

(9) Perdew, J. P.; Chevary, J. A.; Vosko, S. H.; Jackson, K. A.; Pederson, M. R.; Singh, D. J.; Fiolhais, C. *Phys. Rev. B* **1992**, *46*, 6671.

(10) Ghosh, A. *Acc. Chem. Res.* **1998**, *31*, 189.

(11) (a) Vangberg, T.; Ghosh, A. *J. Phys. Chem. B* **1997**, *101*, 1496. (b) Baker, J.; Kozlowski, P. M.; Jarzecki, A. A.; Pulay, P. *Theor. Chem. Acc.* **1997**, *97*, 59.

(12) (a) Ghosh, A.; Jynge, K. *J. Phys. Chem. B* **1997**, *101*, 5459. (b) Wu, Y. D.; Chan, K. W. K.; Yip, C. P.; Vogel, E.; Plattner, D. A.; Houk, K. N. *J. Org. Chem.* **1997**, *62*, 9240. (c) Vogel, E.; Bröring, M.; Plattner, D. A.; Nendel, M.; Houk, K. N. *Angew. Chem., Int. Ed. Engl.* **1995**, *34*, 2511.

(13) Ghosh, A.; Jynge, K. *Chem. Eur. J.* **1997**, *3*, 823.

(14) Ghosh, A. *J. Phys. Chem. B* **1997**, *101*, 3290.

(15) (a) Vangberg, T.; Ghosh, A. *J. Am. Chem. Soc.* **1998**, *120*, 6227. (b) Ghosh, A.; Vangberg, T. *Theor. Chem. Acc.* **1997**, *97*, 143.

(16) (a) Ghosh, A. *J. Phys. Chem.* **1994**, *98*, 11004. (b) Ghosh, A. *J. Am. Chem. Soc.* **1995**, *117*, 4691. (c) Ghosh, A. *J. Mol. Struct. (Theochem)* **1996**, *388*, 359.

(17) Molecule **4** has been previously studied at the B3LYP/6-31G**// B3LYP/6-31G level and its energy was found to be 4.6 kcal/mol above **1**: Szterenberg, L.; Latos-Grazynski, L. *Inorg. Chem.* **1997**, *36*, 6287.

(18) For an NL-DFT optimized structure of porphyrin, see Figure 4 in ref 15b.

(19) (a) Arduengo, A. J., III; Harlow, R. L.; Kline, M. *J. Am. Chem. Soc.* **1991**, *113*, 361. (b) *J. Phys. Chem.* **1991**, *95*, 4180.

(20) Lavorato, D.; Terlouw, J. K.; Dargel, T. K.; Koch, W.; McGibbon, G. A.; Schwarz, H. *J. Am. Chem. Soc.* **1996**, *118*, 11898.

(21) Lash, T. D.; Chaney, S. T. *Angew. Chem., Int. Ed. Engl.* **1997**, *36*, 839.

(22) Lee, C. H.; Kim, H. J. *Tetrahedron Lett.* **1997**, *38*, 3935.

(23) Ishikawa, Y.; Yoshida, I.; Akaiwa, K.; Koguchi, E.; Sasaki, T.; Furuta, H. *Chem. Lett.* **1997**, 453.